

# SSR: A Generic Framework for Text-Aided Map Compression for Localization

Mohammad Omama<sup>1</sup>, Po-han Li<sup>1</sup>, Harsh Goel<sup>1</sup>, Minkyu Choi<sup>1</sup>, Behdad Chalaki<sup>2</sup>,  
Vaishnav Tadiparthi<sup>2</sup>, Hossein Nourkhiz Mahjoub<sup>2</sup>, Ehsan Moradi Pari<sup>2</sup>, Sandeep P. Chinchali<sup>1</sup>

<sup>1</sup>The University of Texas at Austin, <sup>2</sup>Honda Research Institute

## Abstract:

Mapping is crucial in robotics for localization and downstream decision-making. As robots are deployed in ever-broader settings, the maps they rely on continue to increase in size. However, storing these maps indefinitely (cold storage), transferring them across networks, or sending localization queries to cloud-hosted maps imposes prohibitive memory and bandwidth costs. We propose a text-enhanced compression framework that reduces both memory and bandwidth footprints while retaining high-fidelity localization. The key idea is to treat text as an alternative modality—one that can be losslessly compressed with large language models. We propose leveraging lightweight text descriptions combined with very small image feature vectors, which capture “*complementary information*” as a compact representation for the mapping task. Building on this, our novel technique, Similarity Space Replication (SSR), learns an adaptive image embedding in one shot that captures only the information “*complementary*” to the text descriptions. We validate our compression framework on multiple downstream localization tasks, including Visual Place Recognition as well as object-centric Monte-Carlo localization in indoor as well as outdoor settings. SSR achieves 2× better compression than competing baselines on state-of-the-art datasets, including TokyoVal, Pittsburgh30k, Replica, and KITTI.

**Keywords:** Compression, Mapping, Localization

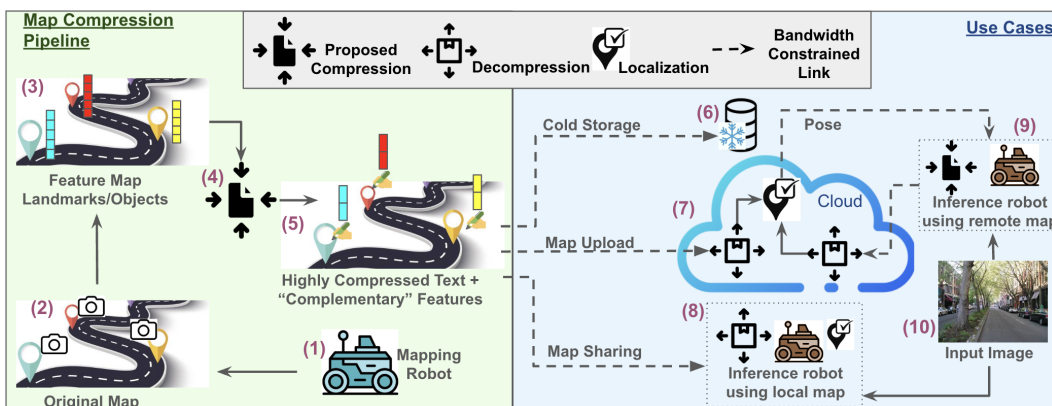


Figure 1: **Map compression pipeline and downstream use-cases.** The mapping robot (1) first creates a standard map of the environment (2), which is then converted into a feature map (3). Our proposed compression framework (4) processes these feature maps into highly compressed text and complementary feature vectors (5). The compressed map can be stored in cold storage (6), uploaded to a server (7) for remote queries, or transmitted to another robot (8). During inference, if the robot has the compressed map locally (8), standard localization is performed. Otherwise, the input image (10) is compressed by the robot (9), sent to the server, decompressed, and localized, with the resulting pose returned to the robot.

# 1 Introduction

Modern robots—like self-driving cars, delivery drones, and warehouse vehicles—localize by matching live sensory input against *ever-growing maps*. These maps grow continuously as robots are deployed to new areas. In city-scale ride-hailing systems, for example, the landmark database can exceed terabytes of data. Sending daily map updates to hundreds of cars can overwhelm cellular networks. Bandwidth and storage constraints appear in other settings as well. An indoor service robot frequently sends image snippets to a cloud server that hosts a high-resolution map of its operational area; each query incurs both latency and bandwidth costs. Further, survey drones that fly week-long missions over farmland collect petabytes of imagery; archiving this data for later use has prohibitive memory costs. All of these scenarios underline a simple point: without effective compression techniques, map storage and communication quickly become the dominant costs in robotic localization. Consequently, there

is a pressing need for map compression techniques tailored for localization that **a) reduce memory and bandwidth footprints** and **b) seamlessly adapt to varying resource constraints**.

To address this, we propose a novel map compression pipeline (illustrated in Fig. 1), which transforms feature maps into highly compressed text descriptions and complementary feature vectors, enabling efficient storage, transmission, and localization across diverse deployment settings. Existing classical and neural compression techniques focus on reconstruction quality, making them unsuitable for localization. Other popular map compression techniques primarily focus on dimensionality reduction or quantization.

Contrastingly, our approach, leverages lightweight, easily-compressible text descriptions generated by vision-language models, combined with compact image feature vectors. These compact feature vectors are learned using our novel method, Similarity Space Replication (SSR), and capture “complementary information”. Together, the text descriptions and complementary image vectors enable a compact solution for map compression tailored for localization. Fig. 2 shows a Visual Place Recognition (VPR) scenario where the goal is to find the closest match for a query image of a building. Text descriptions can easily eliminate the bottom two candidates in the reference set, but fail to distinguish between the top two. By integrating text with “complementary features”—like whether the building tapers—we accurately identify the correct match using minimal data. Moreover, our approach SSR is adaptive and does not require separate training to adapt to fluctuating bandwidth.

**Motivation for Using Text:** Our two key insights are that text is inherently more compact and significantly easier to compress than images or feature vectors. For example, a JPEG image [1] is typically around 500 KB, while a CLIP feature vector [2] is approximately 4 KB. In contrast, a concise 1–2 line caption describing the image is roughly 0.1 KB. Moreover, leveraging recent advancements such as LLMZip [3], the caption can be further compressed losslessly—down to approximately 0.025 KB—making text an ideal modality for compression. As a result, we only need marginal or complementary information from the image, which we obtain using our novel technique, SSR. To the best of our knowledge, this is the first work to demonstrate that recent LLM-based compression techniques can be extended to robotic map compression.

The central idea of this work is presented in Fig. 3. To summarize, our contributions are:

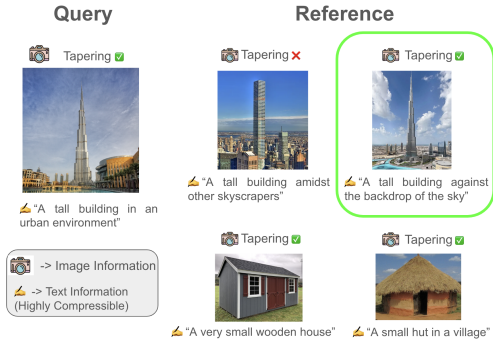


Figure 2: **Highly compressible text descriptions combined with “complementary” image information are enough for effective localization.** Text descriptions (highly compressible) are good enough to discard the bottom two candidates in the reference set for the given query but struggle to distinguish between the top two. Integrating complementary details from the image, like whether the building tapers, ensures a precise match.

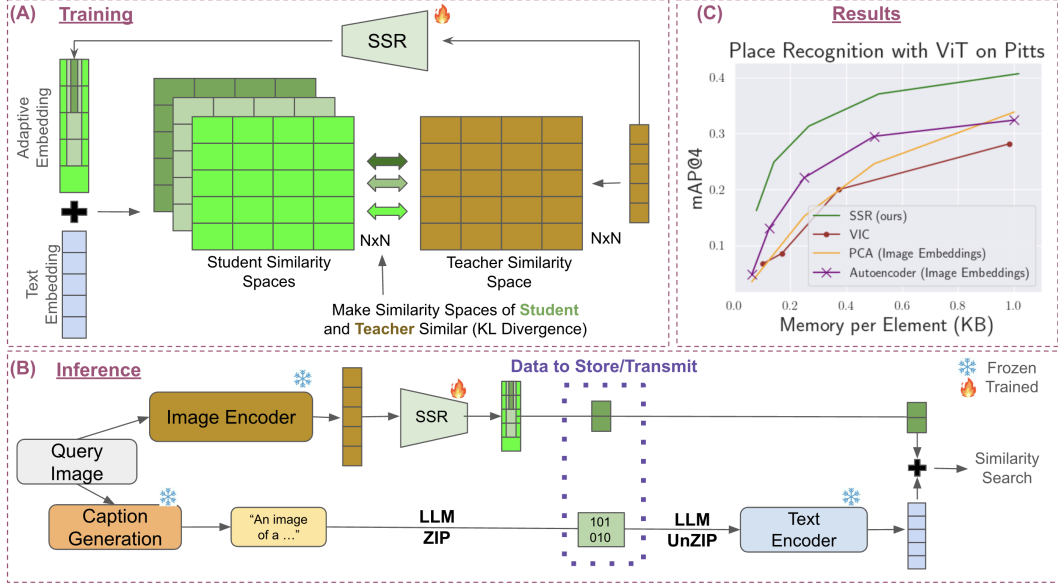


Figure 3: **Pipeline for SSR.** (A) SSR (detailed in Sec. 3.3) learns adaptive embeddings (green) from the image embeddings (brown) that capture complementary information to the text embeddings (blue). (B) During inference, SSR projects the image embedding to any desired dimension based on the constraints. In parallel, captions are generated (Sec. 3.1) and then compressed with LLMZip (Sec. 3.2). The projected complementary feature vector and LLMZipped text are then stored or transmitted. (C) SSR (green) outperforms all competing compression baselines (complete results in Sec. 4.2).

1. We propose a novel technique that uses text, highly compressed with LLMZip, and complementary image information to achieve effective map compression.
2. Our method, Similarity Space Replication (SSR), effectively learns an adaptive embedding that captures information complementary to text, as shown in Fig. 3(A) and further discussed in Sec. 3.3. SSR can work with any feature extractor as demonstrated in Sec. 4.2.
3. Our approach achieves  $2\times$  better compression than competing baselines on state-of-the-art (SOTA) localization datasets, as shown in Fig. 3(C) and discussed in Sec. 4.2. We also release our codebase in the supplementary material.

Throughout the paper, when we refer to SSR in the context of methodology, we mean our approach for learning complementary image feature factors, as illustrated in Fig. 3(A). In the context of experiments, these terms denote the complete compression setup, incorporating both the complementary image feature vectors and the LLMZipped text during inference as shown in Fig. 3(B).

## 2 Background and Related Work

**Deep Metric Learning:** Deep Metric Learning (DML) provides a foundation for image retrieval [4], focusing on generating latent representations where similar items are positioned closely in the embedding space, while dissimilar items are pushed apart. Numerous techniques have been developed [5, 6, 7, 8, 9, 10, 11] to create these representations, leveraging strategies like contrastive loss [12], triplet loss [6], advanced N-pair loss [8], and multi-similarity loss [9]. Similarly, VPR applies DML principles to embed images in a way that clusters similar locations together while distancing unrelated ones [13]. For VPR, specific training objectives have been designed [14, 15, 16, 17] to enhance retrieval capabilities by refining these embeddings to improve the clustering of like locations and the separation of distinct ones. Furthermore, composed retrieval [18, 19] involves using a combination of text, images, and sketches to retrieve images. However, while these approaches focus on learning effective latent representations for retrieval tasks, they do not address the challenge of compression, particularly in a localization setting.

**Image Compression Techniques:** Traditional image compression methods, such as JPEG [1] and JPEG2000 [20], rely on mathematical transformations and quantization processes to reduce file sizes while preserving visual quality. Advancements in Deep Learning (DL) have led to more effective image compression methods [21, 22]. Autoencoders (AEs) are popular for this task [23], and Variational Autoencoders (VAEs) extend AEs with a probabilistic framework for more flexible latent representations [24]. Generative adversarial networks (GANs) further enhance perceptual quality in image reconstruction [25]. Recent methods also use arithmetic encoding for more efficient latent space compression [26, 27]. Additionally, quantization techniques reduce file sizes by mapping pixel values or latent representations to finite sets [28]. However, these methods are generally reconstruction-focused, rather than optimized for retrieval. For retrieval-oriented compression, methods typically employ autoencoders [24] or PCA [29] for dimensionality reduction of the feature vector used in retrieval, or quantization [30] to reduce its size. These methods, however, tend to degrade performance significantly at higher compression levels. In contrast, SSR introduces a novel approach that leverages text captions, combined with complementary image embeddings, to enable memory-optimized retrieval.

**Vision Language Models (VLMs):** VLMs such as InternVL [31], LLaVA [32], BLIP-2 [33] and InstructBlip [34] have gained popularity in recent years for tasks such as VQA, multi-modal dialogue generation, image captioning, etc. We leverage these recent advancements and apply them in the image retrieval domain by relying on the zero-shot image captioning capabilities of VLMs.

**Similarity Preserving Knowledge Distillation:** Much like traditional distillation techniques [35, 36, 37, 38, 39, 40], similarity-preserving knowledge distillation (SPKD) focuses on transferring knowledge from a teacher model to a student model while ensuring that the similarity relationships between data points in the feature space are retained. FitNets [41] guide the student model using the teacher’s intermediate features, while attention transfer aligns attention maps [38]. Pairwise similarity preservation [42], Relational Knowledge Distillation (RKD) [43], and Contrastive Representation Distillation (CRD) [44] retain data relationships, with CRD using contrastive loss to maximize mutual information. We adapt SPKD to generate “complementary” embeddings from image feature extractors. These embeddings, when combined with text embeddings, preserve the original feature extractor’s similarity relationships.

**Adaptive Feature Embeddings:** A fundamental challenge in representation learning is the need for adaptive embedding sizes to accommodate different compute/memory limits. Prior works have developed adaptive feature embeddings for tasks such as reconstruction [45] and classification [46]. In contrast, our approach learns adaptive embeddings for localization-focused map compression.

## 3 Methodology

### 3.1 Caption Generation Using Vision-Language Models

Our approach requires a modality switch, necessitating a caption generation module, for which any suitable VLM could be used. We use a VLM called LLaVA (Large Language and Vision Assistant) [32], a multimodal framework that integrates Large Language Models (LLMs) with visual encoders to enable image-captioning capabilities. LLaVA generates detailed, context-rich captions using a Vision Transformer (ViT) to extract image features, which are then interpreted by an LLM to create descriptions. In our experiments, we employ the LLaVA-1.3B model and consistently use the prompt “describe the image in two lines” to guide caption generation. While we can use any caption generation model, using LLaVA provides unique benefits. As a foundation model, LLaVA is versatile and can be applied across diverse datasets without retraining. Additionally, being based on an LLM, LLaVA brings further advantages like LLM-based compression as discussed in Sec. 3.2.

### 3.2 Extreme Lossless Text Compression

With the rise of LLMs, new lossless extreme text compression techniques have emerged, making text an ideal modality for efficient compression. In this context, we leverage LLMZip [3], a SOTA

compression method that harnesses the power of LLMs to perform lossless text compression. By utilizing the predictive capabilities of these models, LLMZip encodes text more efficiently, transforming token predictions into highly compact bit representations. LLMZip requires some LLM to work with. It was originally designed for LLaMA-7B [47]. Since we are already using LLaVA for captioning and LLaVA is based on an LLM, we directly integrate it with the LLMZip framework, eliminating the need for an additional LLM for probability predictions. Following LLMZip’s pipeline, LLaVA’s generated captions undergo tokenization and probability estimation, with predicted tokens ranked by likelihood and compressed using arithmetic coding. By using LLMZip in the loop, a lot of information can be stored or transmitted as highly compressed text while only some additional information is needed from the image vectors.

### 3.3 Learning Complementary Information Using Similarity Space Replication (SSR)

**Overview:** Fig. 3(A) illustrates the central idea behind SSR. Let  $z \in \mathbb{R}^d$  represent the full image embedding vector generated from any feature extractor of choice. Our goal is to reduce the dimensionality of  $z$  such that the performance of this reduced embedding, when combined with the text embedding, approximates that of the full image embedding. In essence, the complete image embedding  $z$  guides the creation of a smaller, “complementary” image embedding. The key insight is that the complete image embedding is well-suited for localization tasks. We create a similarity space based on this complete embedding, represented by an  $N \times N$  similarity matrix, where  $N$  is the number of elements in the database. We then construct a comparable similarity space using the “complementary” embedding in conjunction with the text embedding. Our objective is to ensure that the latter similarity space closely approximates the former. To achieve this, we introduce a Kullback-Leibler (KL) divergence loss between the two similarity matrices, similar to [48], which we refer to as the Similarity Space Replication loss. An important aspect of our approach is adaptability to varying bandwidth and memory constraints. Rather than training separate SSR models for each possible embedding dimension, we train a single SSR model that can produce adaptive embeddings by following the approach in [46], and optimizing the Similarity Space Replication loss across each nested dimension. This flexibility allows us to select any number of dimensions from the embedding, with each selection providing an effective trade-off between performance and memory.

**Approach:** Let  $\mathcal{C} \subset [d]$  represent a collection of embedding dimensions and define a neural network  $\mathcal{G}(\cdot; \phi)$  with parameters  $\phi$ . The objective is to learn a mapping  $\hat{z} = \mathcal{G}(z; \phi)$  such that each of the first  $c$  dimensions, for  $c \in \mathcal{C}$ , of the resulting embedding vector  $\hat{z}^{1:c} \in \mathbb{R}^c$  maintains performance for  $z$  when combined with the text embedding  $z_{\text{text}}$ .

We first calculate a cosine similarity matrix  $\mathcal{S} \in \mathbb{R}^{N \times N}$  by evaluating the cosine similarities between each pair of  $z$  in the database. We term this matrix the cosine similarity space of the reference embeddings  $Z$  or the “teacher similarity space” as shown in Fig. 3(A). Let  $\mathcal{S}_j$  represent the  $j^{\text{th}}$  row of  $\mathcal{S}$ . For each  $c \in \mathcal{C}$ , we define a “student similarity space”  $\tilde{\mathcal{S}}^c \in \mathbb{R}^{N \times N}$  by combining  $\hat{z}^{1:c}$  with the text feature vector  $z_{\text{text}}$ . We then use the KL divergence loss  $l^c$  between  $\tilde{\mathcal{S}}^c$  and  $\mathcal{S}$  for each  $c$  as:

$$l^c = \sum_{j=1}^N D_{\text{KL}}(\tilde{\mathcal{S}}_j^c \| \mathcal{S}_j). \quad (1)$$

The total loss  $L$  is expressed as:

$$L_{\text{SSR}} = \sum_{c \in \mathcal{C}} l^c = \sum_{c \in \mathcal{C}} \sum_{j=1}^N D_{\text{KL}}(\tilde{\mathcal{S}}_j^c \| \mathcal{S}_j). \quad (2)$$

### 3.4 Applying SSR in Different Localization Settings

SSR can be seamlessly applied to VPR settings by captioning each image to obtain the corresponding text description. In this case, the number of database elements  $N$  equals the number of images in the VPR database. For object-centric localization, we introduce a minor adaptation to the SSR pipeline. Recent object-centric Monte-Carlo localization approaches, like ConceptGraphs [49] and

Sparseloc [50], extract object embeddings from multiple viewpoints and fuse them during the mapping process. Following [49], we generate object captions by first cropping the object from each viewpoint and passing the crops to a captioning model. We then prompt the VLM to synthesize a unified caption across all viewpoints. In this setting,  $N$  corresponds to the number of distinct objects in the map. The remainder of the map compression pipeline remains unchanged.

**Multi-robot Settings:** In Appendix A.2, we demonstrate that our compression pipeline can be seamlessly extended to multi-robot federated learning settings. Our approach outperforms other methods in a federated setup, due to its better data efficiency, as further discussed in Appendix A.3.

## 4 Experiments

### 4.1 Experimental Setup

**Datasets:** We validate our compression framework across multiple downstream localization tasks, including visual place recognition and object-centric Monte Carlo localization, in both indoor and outdoor environments. For visual place recognition, we report results on the Pittsburgh30K [51] and TokyoVal [52] datasets. For object-centric Monte Carlo localization, we present results on the Replica [53] (indoor) and KITTI [54] (outdoor) datasets.

**Feature Extractors Evaluated:** To demonstrate that our approach is applicable with any choice of feature vector used for localization, we conducted experiments using three different feature extractors, each pre-trained with different datasets and techniques: DINO [55], DINOv2 [56], and ViT [57]. The ViT and DINO models were both pre-trained in a self-supervised manner on the ImageNet dataset [58], while the DINOv2 model was trained on the LVD-142M dataset [59]. These feature vectors are used as teachers to train the SSR model as discussed in Sec. 3.3.

**Settings:** For the visual place recognition tasks, we evaluate retrieval performance across different compression levels for each approach. Retrieval performance is measured using mean Average Precision at  $k$  (mAP@ $k$ ), a standard metric for retrieval evaluation. Additional results based on the Recall@ $k$  metric are provided in Appendix A.5. For object-centric Monte Carlo localization, we evaluate localization performance using the absolute position error (APE) metric across different compression levels. For compression, we measure the memory per element (i.e., per image) transferred over the bandwidth in its compressed form, reported in kilobytes (KB). Our approach, SSR, transmits an LLMZipped text description along with a complementary image feature vector. As discussed in Section 3.3, the size of this feature vector is adaptable, allowing selection of any number of dimensions based on bandwidth or memory constraints. The total memory per element in our approach is the sum of the complementary vector’s size (depending on the selected number of dimensions) and the size of the LLMZipped text.

**Baselines:** We compare three main categories of baselines. The first two categories are specifically tailored for VPR, while the third category is more general and can be applied to both VPR and object-centric Monte Carlo localization. The first category includes classical compression techniques, such as **JPEG** [1] and **JPEG2000** [20]. The second category includes neural network-based compression methods focused on image reconstruction, such as Variational Image Compression (**VIC**) [27] and Gaussian Mixture Likelihoods (**GML**) [26]. In both these categories, we assume that the query image is compressed locally, transmitted to the server, decompressed, and subsequently used for feature extraction. For JPEG and JPEG2000, the memory per element is simply the size of the compressed image (in KB) in the respective format. For neural network-based methods, the memory per element corresponds to the size of the compressed latent representation (in KB), which is decompressed on the server side for feature extraction. The third category assumes feature extraction is performed locally, followed by compression of the extracted features using dimensionality reduction techniques. We evaluate the following baselines in this category:

1. **PCA (Image Embedding):** Image feature vectors are generated for localization and then compressed using PCA. The memory per element is the size of the PCA-compressed embedding.

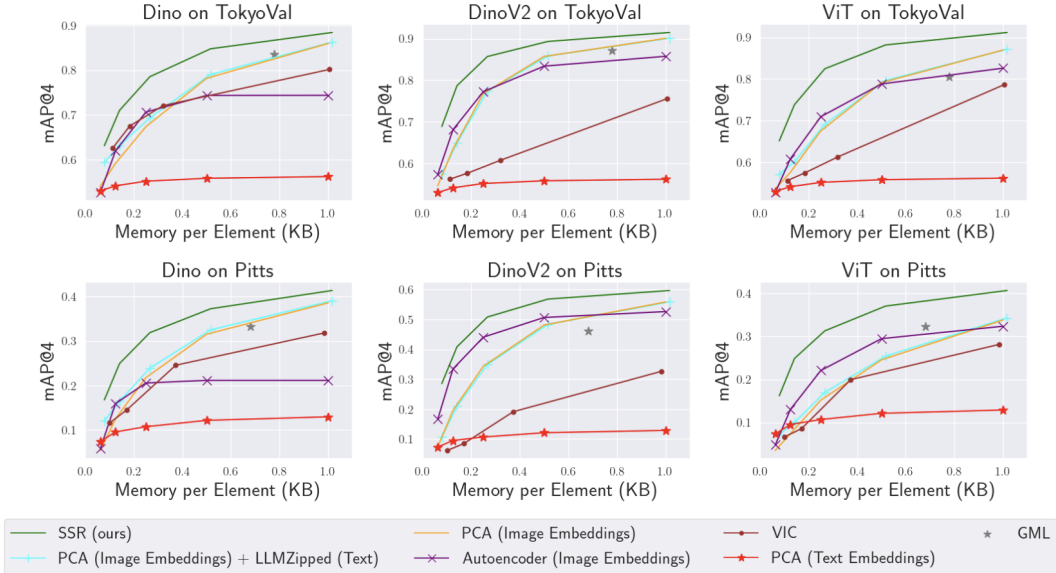


Figure 4: **SSR is highly effective for map compression in VPR settings** We show the place recognition performance of all approaches across various compression levels on the TokyoVal and Pittsburgh datasets, using Dino, DinoV2, and ViT embeddings. SSR (green) consistently outperforms all baselines, particularly at smaller memory footprints.

2. **Autoencoder (Image Embedding)**: Image feature vectors are generated for localization and then compressed using an Autoencoder. The memory per element is the size of the Autoencoder-compressed embedding.
3. **PCA (Text Embedding)**: An image caption is generated, its embedding is obtained, which is then compressed using PCA. The memory per element is the size of the PCA-compressed text embedding.
4. **PCA (Image Embedding) + LLMZipped (Text)**: Image feature vectors are generated and compressed using PCA. In addition, image captions are generated and compressed using LLMZip. The total memory per element is the sum of the PCA-compressed image vector size and the LLMZipped text size. On the server side, the text is decompressed, its feature vector is generated, concatenated with the PCA-compressed image vector, and used for localization.

We further evaluate other feature vector compression techniques like quantization in this category. Our approach, however, transmits LLMZipped text data with a negligible memory footprint combined with a small complementary image vector. This setup renders all feature vector compression techniques (like quantization, etc.) orthogonal to our method, as the same compression techniques can be applied to the complementary small image vector while the LLMZipped text data has a near-negligible memory footprint. We discuss this in Appendix A.4

## 4.2 Results

In Fig. 4, we compare SSR against the baselines discussed in Sec. 4.1 for the **VPR** task. Note that the performance of JPEG and JPEG2000 was poor; therefore, we omit these results from the main text but include them in Appendix A.6. The rows in Fig. 4 correspond to different datasets, while the columns represent various feature extractors, as described in Sec. 4.1. Our goal is to demonstrate that our approach is compatible with any dataset and feature extractor used for localization. SSR (green) consistently outperforms all baselines across all scenarios, achieving on average  $2\times$  better compression than competing baselines. For example, on the Pittsburgh30K dataset with ViT embeddings, SSR achieves a performance of 0.34 mAP with a memory footprint of only 0.4 KB, whereas the closest baseline, Autoencoders (magenta), requires approximately 1 KB per element.

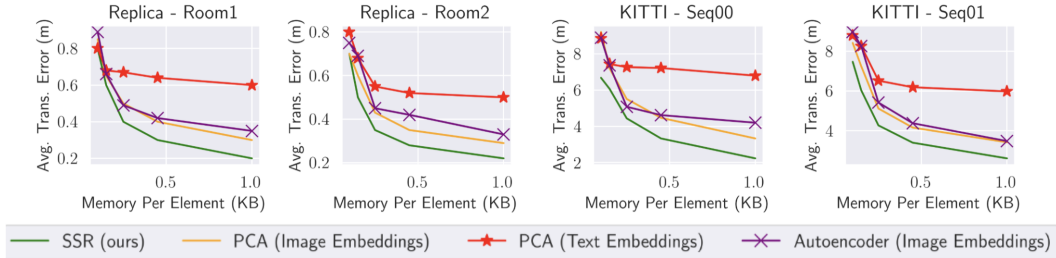


Figure 5: SSR **generalizes effectively to Monte Carlo localization tasks**. We show the localization performance (absolute position error) of all approaches across various compression levels on two Replica rooms and two KITTI sequences. SSR (green) consistently achieves lower localization error than competing baselines.

Interestingly, we trained different Autoencoder models for each compression level (dimension size). In contrast, for SSR we only had to train a single model and then select any desired dimension size at inference, as discussed in Sec. 3.3. The results also show that the second category of baselines (VIC (brown) and GML (gray)) perform poorly, as they focus on image reconstruction rather than similarity search. Moreover, GML results are shown only for specific compression levels, as it is not easily adaptable to varying compression ratios. Finally, SSR surpasses both PCA and Autoencoders in the third category of baselines, highlighting its optimization specifically for localization tasks. Another notable baseline is “PCA (Image Embedding) + LLMZipped (Text)” (cyan), which is structurally similar to our method: transmitting a compressed text description along with a complementary image feature vector. However, SSR significantly outperforms this baseline, emphasizing the value of *learning* complementary image information rather than relying on independent compression pipelines. Since VPR is an image retrieval problem, our approach also applies to general image retrieval datasets, as discussed in Appendix A.1.

In Fig. 5, we evaluate SSR on object-centric Monte Carlo localization tasks. We present results on two indoor scenes from the Replica dataset (Room0 and Room1) and two outdoor sequences from the KITTI dataset (Seq00 and Seq01). For this task, we focus exclusively on the third category of baselines — those based on feature compression rather than full image compression. This is because object-centric mapping extracts object crops using approaches such as SAM [60], obtains their features, and fuses features from multiple viewpoints. Baselines like VIC and GML cannot be extended to this setting. Note that we use DINO for object feature extraction to remain consistent with [50, 49], although any feature extractor can be used. The performance is measured in terms of absolute position error (APE) across varying compression levels. Consistent with the VPR results, SSR, outperforms traditional PCA- and Autoencoder-based approaches, demonstrating that our method generalizes effectively to downstream localization tasks beyond retrieval.

## 5 Conclusion, Limitations, and Future Work

In this paper, we proposed SSR that uses text as an alternative modality that captures information complementary to the image data. It achieves  $2\times$  better compression than competing baselines. Although SSR saves memory and bandwidth, it is computationally intensive. During inference, it runs a VLM to generate captions and then LLMZip and a text encoder to compress the text to embeddings, as shown in Fig. 3(B). Thus, SSR offers a trade-off between computation, memory, and bandwidth. Also, since SSR is based on VLMs and the compressibility of text, it cannot extend to other modalities lacking VLMs, such as inertial measurement units. Future works include extending our text-based compression technique to support additional vision tasks beyond localization, such as joint image and text compression and reconstruction. Another area is to optimize LLM prompts [61] to generate captions that fully capture the visual information in images, thus we can completely discard image embeddings in our compression framework.

## References

- [1] G. K. Wallace. The jpeg still picture compression standard. *Communications of the ACM*, 34(4):30–44, 1991.
- [2] A. Radford, J. W. Kim, C. Hallacy, A. Ramesh, G. Goh, S. Agarwal, G. Sastry, A. Askell, P. Mishkin, J. Clark, et al. Learning transferable visual models from natural language supervision. In *International conference on machine learning*, pages 8748–8763. PMLR, 2021.
- [3] C. S. K. Valmeekam, K. Narayanan, D. Kalathil, J.-F. Chamberland, and S. Shakkottai. Llmzip: Lossless text compression using large language models. *arXiv preprint arXiv:2306.04050*, 2023.
- [4] J. Wang, Y. Song, T. Leung, C. Rosenberg, J. Wang, J. Philbin, B. Chen, and Y. Wu. Deep metric learning: A survey. *arXiv preprint arXiv:1706.09720*, 2017.
- [5] H. Oh Song, Y. Xiang, S. Jegelka, and S. Savarese. Deep metric learning via lifted structured feature embedding. In *Proceedings of the IEEE conference on computer vision and pattern recognition*, pages 4004–4012, 2016.
- [6] F. Schroff, D. Kalenichenko, and J. Philbin. Facenet: A unified embedding for face recognition and clustering. In *Proceedings of the IEEE conference on computer vision and pattern recognition*, pages 815–823, 2015.
- [7] E. Ustinova and V. Lempitsky. Learning deep embeddings with histogram loss. *Advances in neural information processing systems*, 29, 2016.
- [8] K. Sohn. Improved deep metric learning with multi-class n-pair loss objective. *Advances in neural information processing systems*, 29, 2016.
- [9] X. Wang, X. Han, W. Huang, D. Dong, and M. R. Scott. Multi-similarity loss with general pair weighting for deep metric learning. In *Proceedings of the IEEE/CVF conference on computer vision and pattern recognition*, pages 5022–5030, 2019.
- [10] M. Omama, P.-h. Li, and S. P. Chinchali. Exploiting distribution constraints for scalable and efficient image retrieval. *arXiv preprint arXiv:2410.07022*, 2024.
- [11] P.-h. Li, S. P. Chinchali, and U. Topcu. Csa: Data-efficient mapping of unimodal features to multimodal features. *arXiv preprint arXiv:2410.07610*, 2024.
- [12] R. Hadsell, S. Chopra, and Y. LeCun. Dimensionality reduction by learning an invariant mapping. In *2006 IEEE computer society conference on computer vision and pattern recognition (CVPR'06)*, volume 2, pages 1735–1742. IEEE, 2006.
- [13] S. Garg, T. Fischer, and M. Milford. Where is your place, visual place recognition? In *IJCAI*, volume 8, pages 4416–4425, 2021.
- [14] Y. Ge, H. Wang, F. Zhu, R. Zhao, and H. Li. Self-supervising fine-grained region similarities for large-scale image localization. In *Computer Vision—ECCV 2020: 16th European Conference, Glasgow, UK, August 23–28, 2020, Proceedings, Part IV 16*, pages 369–386. Springer, 2020.
- [15] J. Xiao, G. Zhu, and G. Loianno. Visual geo-localization with self-supervised representation learning. *arXiv preprint arXiv:2308.00090*, 2023.
- [16] M. Leyva-Vallina, N. Strisciuglio, and N. Petkov. Data-efficient large scale place recognition with graded similarity supervision. In *Proceedings of the IEEE/CVF Conference on Computer Vision and Pattern Recognition*, pages 23487–23496, 2023.

- [17] G. Berton, C. Masone, and B. Caputo. Rethinking visual geo-localization for large-scale applications. In *Proceedings of the IEEE/CVF Conference on Computer Vision and Pattern Recognition*, pages 4878–4888, 2022.
- [18] H. Ge, Y. Jiang, J. Sun, K. Yuan, and Y. Liu. Llm-enhanced composed image retrieval: An intent uncertainty-aware linguistic-visual dual channel matching model. *ACM Trans. Inf. Syst.*, Oct. 2024. ISSN 1046-8188. doi:10.1145/3699715. URL <https://doi.org/10.1145/3699715>. Just Accepted.
- [19] Z. Yang, D. Xue, S. Qian, W. Dong, and C. Xu. Ldre: Llm-based divergent reasoning and ensemble for zero-shot composed image retrieval. In *Proceedings of the 47th International ACM SIGIR Conference on Research and Development in Information Retrieval, SIGIR '24*, page 80–90, New York, NY, USA, 2024. Association for Computing Machinery. ISBN 9798400704314. doi:10.1145/3626772.3657740. URL <https://doi.org/10.1145/3626772.3657740>.
- [20] A. Skodras, C. Christopoulos, and T. Ebrahimi. Jpeg 2000 image coding system: digital compression for still images. *IEEE Transactions on Consumer Electronics*, 46(4):919–929, 2001.
- [21] D. Mishra, S. K. Singh, and R. K. Singh. Deep architectures for image compression: a critical review. *Signal Processing*, 191:108346, 2022.
- [22] S. Ma, X. Zhang, C. Jia, Z. Zhao, S. Wang, and S. Wang. Image and video compression with neural networks: A review. *IEEE Transactions on Circuits and Systems for Video Technology*, 30(6):1683–1698, 2019.
- [23] L. Theis, W. Shi, A. Cunningham, and F. Huszár. Lossy image compression with compressive autoencoders. *arXiv preprint arXiv:1703.00395*, 2017.
- [24] D. P. Kingma and M. Welling. Auto-encoding variational bayes. *arXiv preprint arXiv:1312.6114*, 2013.
- [25] E. Agustsson, M. Tschannen, F. Mentzer, R. Timofte, and L. Van Gool. Generative adversarial networks for extreme learned image compression. In *Proceedings of the IEEE International Conference on Computer Vision Workshops (ICCVW)*, pages 221–231, 2019.
- [26] Z. Cheng, H. Sun, M. Takeuchi, and J. Katto. Learned image compression with discretized gaussian mixture likelihoods and attention modules, 2020. URL <https://arxiv.org/abs/2001.01568>.
- [27] J. Ballé, D. Minnen, S. Singh, S. J. Hwang, and N. Johnston. Variational image compression with a scale hyperprior, 2018. URL <https://arxiv.org/abs/1802.01436>.
- [28] G. Toderici, D. Vincent, N. Johnston, S. J. Hwang, J. Balle, D. Minnen, S. Shor, and M. Covell. Full resolution image compression with recurrent neural networks. In *Proceedings of the IEEE Conference on Computer Vision and Pattern Recognition (CVPR)*, pages 5306–5314, 2016.
- [29] H. Abdi and L. J. Williams. Principal component analysis. *Wiley interdisciplinary reviews: computational statistics*, 2(4):433–459, 2010.
- [30] A. Gersho and R. M. Gray. *Vector quantization and signal compression*, volume 159. Springer Science & Business Media, 2012.
- [31] Z. Chen, J. Wu, W. Wang, W. Su, G. Chen, S. Xing, M. Zhong, Q. Zhang, X. Zhu, L. Lu, et al. Internvl: Scaling up vision foundation models and aligning for generic visual-linguistic tasks. In *Proceedings of the IEEE/CVF Conference on Computer Vision and Pattern Recognition*, pages 24185–24198, 2024.

- [32] H. Liu, C. Li, Q. Wu, and Y. J. Lee. Visual instruction tuning. In A. Oh, T. Naumann, A. Globerson, K. Saenko, M. Hardt, and S. Levine, editors, *Advances in Neural Information Processing Systems*, volume 36, pages 34892–34916. Curran Associates, Inc., 2023. URL [https://proceedings.neurips.cc/paper\\_files/paper/2023/file/6dcf277ea32ce3288914faf369fe6de0-Paper-Conference.pdf](https://proceedings.neurips.cc/paper_files/paper/2023/file/6dcf277ea32ce3288914faf369fe6de0-Paper-Conference.pdf).
- [33] J. Li, D. Li, S. Savarese, and S. Hoi. Blip-2: Bootstrapping language-image pre-training with frozen image encoders and large language models, 2023.
- [34] W. Dai, J. Li, D. Li, A. M. H. Tiong, J. Zhao, W. Wang, B. Li, P. Fung, and S. Hoi. Instructblip: Towards general-purpose vision-language models with instruction tuning, 2023. URL <https://arxiv.org/abs/2305.06500>.
- [35] G. Hinton, O. Vinyals, and J. Dean. Distilling the knowledge in a neural network. *arXiv preprint arXiv:1503.02531*, 2015.
- [36] C. Buciluă, R. Caruana, and A. Niculescu-Mizil. Model compression. In *Proceedings of the 12th ACM SIGKDD international conference on Knowledge discovery and data mining*, pages 535–541, 2006.
- [37] J. Ba and R. Caruana. Do deep nets really need to be deep? In *Advances in neural information processing systems*, pages 2654–2662, 2014.
- [38] S. Zagoruyko and N. Komodakis. Paying more attention to attention: Improving the performance of convolutional neural networks via attention transfer. In *International Conference on Learning Representations (ICLR)*, 2017.
- [39] C. Zhang, S. Bengio, M. Hardt, B. Recht, and O. Vinyals. Your classifier is secretly an energy based model and you should treat it like one. In *International Conference on Learning Representations (ICLR)*, 2019.
- [40] N. Passalis and A. Tefas. Learning deep representations with probabilistic knowledge transfer. In *Proceedings of the European Conference on Computer Vision (ECCV)*, pages 268–284, 2018.
- [41] A. Romero, N. Ballas, S. E. Kahou, A. Chassang, C. Gatta, and Y. Bengio. Fitnets: Hints for thin deep nets. *arXiv preprint arXiv:1412.6550*, 2014.
- [42] F. Tung and G. Mori. Similarity-preserving knowledge distillation. In *Proceedings of the IEEE International Conference on Computer Vision (ICCV)*, 2019.
- [43] W. Park, D. Kim, Y. Lu, and M. Cho. Relational knowledge distillation. In *Proceedings of the IEEE Conference on Computer Vision and Pattern Recognition (CVPR)*, 2019.
- [44] Y. Tian, D. Krishnan, and P. Isola. Contrastive representation distillation. In *International Conference on Learning Representations (ICLR)*, 2020.
- [45] P.-h. Li, S. K. Ankireddy, R. P. Zhao, H. Nourkhiz Mahjoub, E. Moradi Pari, U. Topcu, S. Chinchali, and H. Kim. Task-aware distributed source coding under dynamic bandwidth. *Advances in Neural Information Processing Systems*, 36, 2023.
- [46] A. Kusupati, G. Bhatt, A. Rege, M. Wallingford, A. Sinha, V. Ramanujan, W. Howard-Snyder, K. Chen, S. Kakade, P. Jain, et al. Matryoshka representation learning. *Advances in Neural Information Processing Systems*, 35:30233–30249, 2022.
- [47] H. Touvron, T. Lavril, G. Izacard, X. Martinet, M.-A. Lachaux, T. Lacroix, B. Rozière, N. Goyal, E. Hambro, M. Azhar, A. Rodriguez, A. Joulin, E. Grave, and G. Lample. Llama: Open and efficient foundation language models. *arXiv preprint arXiv:2302.13971*, 2023.

- [48] H. Wu, M. Wang, W. Zhou, H. Li, and Q. Tian. Contextual similarity distillation for asymmetric image retrieval. In *Proceedings of the IEEE/CVF Conference on Computer Vision and Pattern Recognition*, pages 9489–9498, 2022.
- [49] Q. Gu, A. Kuwajerwala, S. Morin, K. Jatavallabhula, B. Sen, A. Agarwal, C. Rivera, W. Paul, K. Ellis, R. Chellappa, C. Gan, C. de Melo, J. Tenenbaum, A. Torralba, F. Shkurti, and L. Paull. Conceptgraphs: Open-vocabulary 3d scene graphs for perception and planning. *arXiv*, 2023.
- [50] P. Paul, V. Bhat, T. Salian, M. Omama, K. M. Jatavallabhula, N. Arulselvan, and K. M. Krishna. Sparseloc: Sparse open-set landmark-based global localization for autonomous navigation. *arXiv preprint arXiv:2503.23465*, 2025.
- [51] A. Torii, J. Sivic, T. Pajdla, and M. Okutomi. Visual place recognition with repetitive structures. In *Proceedings of the IEEE conference on computer vision and pattern recognition*, pages 883–890, 2013.
- [52] A. Torii, R. Arandjelovic, J. Sivic, M. Okutomi, and T. Pajdla. 24/7 place recognition by view synthesis. In *Proceedings of the IEEE conference on computer vision and pattern recognition*, pages 1808–1817, 2015.
- [53] J. Straub, T. Whelan, L. Ma, Y. Chen, E. Wijmans, S. Green, J. Engel, R. Mur-Artal, C. Ren, R. Verma, et al. The replica dataset: A digital replica of indoor spaces. *arXiv preprint arXiv:1906.05797*, 2019.
- [54] A. Geiger, P. Lenz, and R. Urtasun. Are we ready for autonomous driving? the kitti vision benchmark suite. In *Conference on Computer Vision and Pattern Recognition (CVPR)*, 2012.
- [55] M. Caron, H. Touvron, I. Misra, H. Jégou, J. Mairal, P. Bojanowski, and A. Joulin. Emerging properties in self-supervised vision transformers, 2021.
- [56] M. Oquab, T. Darcet, T. Moutakanni, H. Vo, M. Szafraniec, V. Khalidov, P. Fernandez, D. Haziza, F. Massa, A. El-Nouby, M. Assran, N. Ballas, W. Galuba, R. Howes, P.-Y. Huang, S.-W. Li, I. Misra, M. Rabbat, V. Sharma, G. Synnaeve, H. Xu, H. Jegou, J. Mairal, P. Labatut, A. Joulin, and P. Bojanowski. Dinov2: Learning robust visual features without supervision, 2024.
- [57] A. Dosovitskiy, L. Beyer, A. Kolesnikov, D. Weissenborn, X. Zhai, T. Unterthiner, M. Dehghani, M. Minderer, G. Heigold, S. Gelly, J. Uszkoreit, and N. Houlsby. An image is worth 16x16 words: Transformers for image recognition at scale, 2021.
- [58] O. Russakovsky, J. Deng, H. Su, J. Krause, S. Satheesh, S. Ma, Z. Huang, A. Karpathy, A. Khosla, M. Bernstein, et al. Imagenet large scale visual recognition challenge. *International journal of computer vision*, 115:211–252, 2015.
- [59] M. Oquab, T. Darcet, T. Moutakanni, H. V. Vo, M. Szafraniec, V. Khalidov, P. Fernandez, D. Haziza, F. Massa, A. El-Nouby, R. Howes, P.-Y. Huang, H. Xu, V. Sharma, S.-W. Li, W. Galuba, M. Rabbat, M. Assran, N. Ballas, G. Synnaeve, I. Misra, H. Jegou, J. Mairal, P. Labatut, A. Joulin, and P. Bojanowski. Lvd-142m: A curated dataset for self-supervised learning. <https://github.com/facebookresearch/dinov2>, 2023. Utilized in the pre-training of DINOv2 models.
- [60] A. Kirillov, E. Mintun, N. Ravi, H. Mao, C. Rolland, L. Gustafson, T. Xiao, S. Whitehead, A. C. Berg, W.-Y. Lo, et al. Segment anything. *arXiv preprint arXiv:2304.02643*, 2023.
- [61] O. Khattab, K. Santhanam, X. L. Li, D. Hall, P. Liang, C. Potts, and M. Zaharia. Demonstrate-search-predict: Composing retrieval and language models for knowledge-intensive NLP. *arXiv preprint arXiv:2212.14024*, 2022.

## A Appendix

### A.1 Extending SSR to General Image Retrieval Datasets

Since VPR is an image retrieval problem, we can easily show that our proposed solution works well with general image retrieval datasets as well as discussed in Fig. 6.

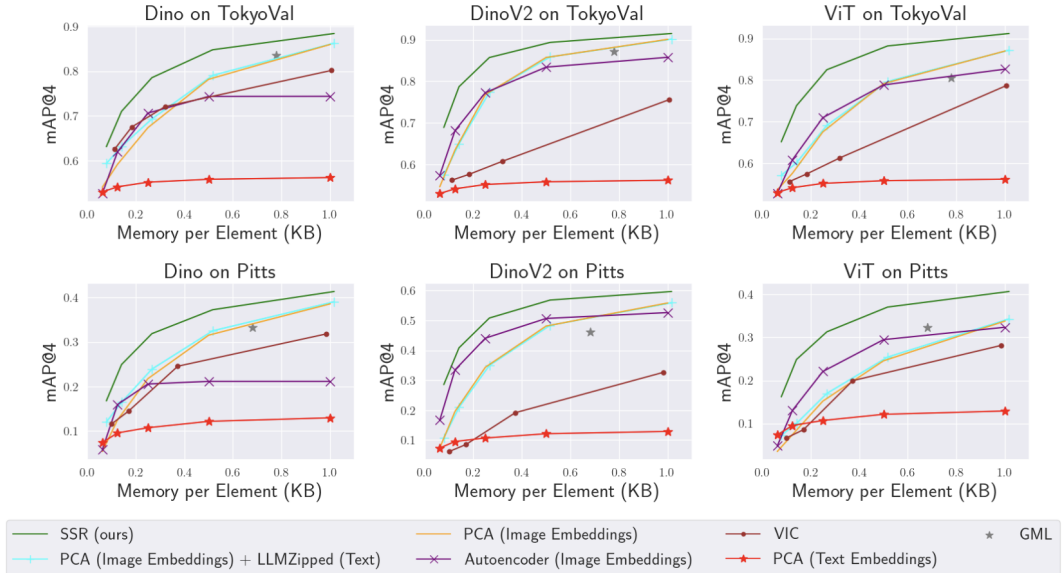


Figure 6: SSR is highly effective for compression in general image retrieval settings as well. We show the image retrieval performance of all approaches across various compression levels on the InShop and SoP datasets, using Dino, DinoV2, and ViT embeddings. SSR (green) consistently outperforms all baselines, particularly at smaller memory footprints.

### A.2 Similarity Space Replication in a Federated Setting (SSR-FL)

**Motivation:** Localization applications often involve privacy-sensitive data distributed across multiple systems. For example, a tourist in a new city may wish to identify landmarks via reverse image search; however, the reference data may be stored across multiple servers managed by different entities, each unwilling to share their proprietary data for training a joint compression function. This scenario introduces both privacy and bandwidth constraints. To address these challenges, we extend Similarity Space Replication (SSR) to a Federated Learning (FL) setup, SSR-FL, enabling privacy-preserving learning of complementary embeddings. SSR-FL meets the requirements of distributed map compression applications by allowing nodes to independently learn and share model updates based on their proprietary data.

**FL Setup:** In our FL setup, we assume there are  $A$  nodes or agents, each with access to its own distinct subset of the training data. These nodes collaborate to train a single SSR-FL model by periodically sharing updates to the model parameters, rather than their raw data. Throughout our experiments, we fix  $A$  to 4 without loss of generality.

**Training Process:** During each training round, each node  $a \in A$  locally optimizes the Similarity Space Replication loss to ensure that its local similarity space, constructed with complementary embeddings, closely approximates the full similarity space. Each node  $a$  individually computes its similarity matrices and complementary embeddings based on its local data, with  $N_a$  images, using the neural network  $\mathcal{G}(\cdot; \phi_a)$ , where  $\phi_a$  represents the model parameters specific to node  $a$ .

For each subset of dimensions  $c \in \mathcal{C}$ , node  $a$  computes the student similarity space  $\tilde{\mathcal{S}}_a^c$  by combining the complementary embeddings  $\hat{z}_a^{1:c}$  with the local text embeddings. The KL divergence loss  $l_a^c$  for

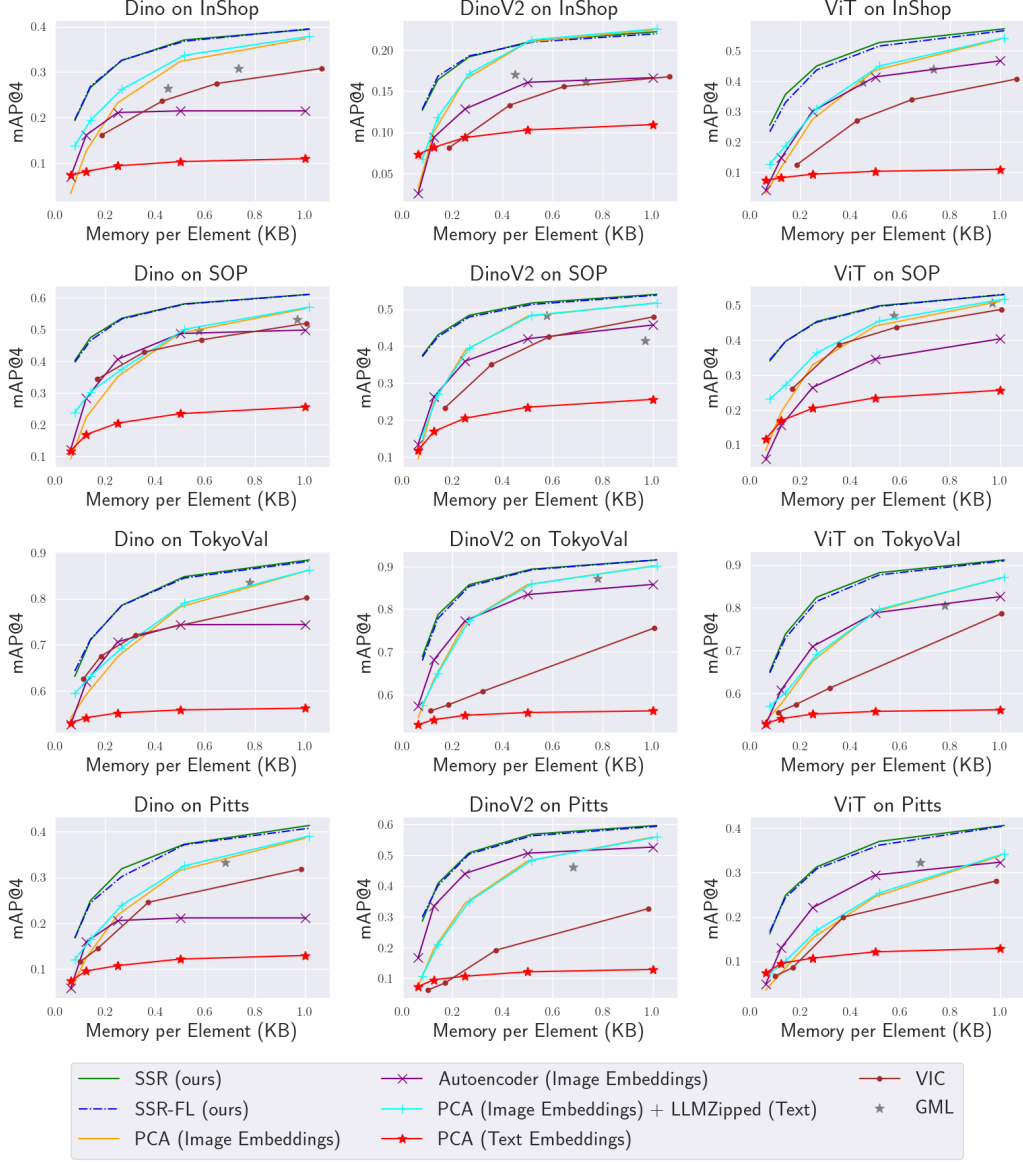


Figure 7: **SSR-FL is as effective as SSR for map compression in VPR settings** We show the place recognition performance of all approaches across various compression levels on the TokyoVal and Pittsburgh datasets, using Dino, DinoV2, and ViT embeddings. SSR (green) consistently outperforms all baselines, while SSR-FL closely approximates SSR.

each dimension subset  $c$  is calculated as:

$$l_a^c = \sum_{j=1}^{N_a} D_{\text{KL}}(\tilde{\mathcal{S}}_{a,j}^c \| \mathcal{S}_{a,j}), \quad (3)$$

where  $\mathcal{S}_a$  denotes the full similarity space computed for node  $a$ . The total loss  $L_a$  for node  $a$  across all embedding dimensions in  $\mathcal{C}$  is given by:

$$L_{\text{SSR}_a} = \sum_{c \in \mathcal{C}} l_a^c = \sum_{c \in \mathcal{C}} \sum_{j=1}^{N_a} D_{\text{KL}}(\tilde{\mathcal{S}}_{a,j}^c \| \mathcal{S}_{a,j}). \quad (4)$$

Each node  $a$  then updates its parameters  $\phi_a$  by minimizing  $L_{\text{SSR}_a}$ . Once these local updates are completed, each node sends its updated parameters  $\phi_a$  to the central server, which aggregates the

updates by averaging them as:

$$\phi = \frac{1}{A} \sum_{a=1}^A \phi_a, \tag{5}$$

where  $A$  is the total number of nodes. The refined global parameters  $\phi$  are then distributed back to each node for the next training round. This iterative process enables our federated SSR-FL model to capture complementary information across different nodes while preserving data privacy.

In the experiments Fig. 7, we show that SSR-FL achieves performance close to SSR, making it well-suited for distributed settings. We argue that this is due to SSR’s training data efficiency, which allows it to be trained in distributed environments efficiently. Since SSR includes an VLM based caption generation, much of the information is already captured in text format, enabling it to focus only on “complementary” information—an easier task than dimensionality reduction via autoencoders, which must learn reconstruction from the ground up. We further compare the data efficiency of SSR and autoencoders in Appendix ??.

### A.3 Data Efficient Training Comparison

In the experiments (Sec. 4.2), we demonstrate that SSR-FL achieves performance comparable to SSR, making it well-suited for distributed settings. This is attributed to SSR’s sample efficiency in learning “complementary image features.” To further illustrate this, we compare the data efficiency of SSR with Autoencoders (AE). Using random small subsets of training data, we analyze the performance drop in VPR (mAP@ $k$ ). The results are summarized in Table 1. Notably, when using only 25% of the training data, the performance of AE drops by 12% (from 0.31 to 0.19), whereas SSR experiences a smaller decline of 6%. These results are shown using the Pittsburgh dataset with the ViT embedding, maintaining a fixed memory per element for both approaches.

We attribute this data efficiency primarily to the use of the VLM-based caption generation, whereby much of the information is already captured in a text format. Therefore, making the learning process of “complementary features” easier.

	AE	SSR
25% Data	0.19	<b>0.31</b>
50% Data	0.22	<b>0.33</b>
75% Data	0.27	<b>0.35</b>
100% Data	0.31	<b>0.37</b>

Table 1: **Performance ( mAP@ $k$ ) comparison between SSR and Autoencoders (AE) when using subsets of training data.** AE shows a 12% performance drop (from 0.31 to 0.19) with 25% training data, while SSR exhibits a smaller drop of 6%.

### A.4 Comparison with Quantization

Additionally, we evaluate quantization in this category. Our approach, however, transmits LLMZipped text data with a negligible memory footprint combined with a small complementary image vector. This setup renders all feature vector compression techniques (like quantization) orthogonal to our method, as the same compression techniques can be applied to the complementary small image vector, while the LLMZipped text data has near near-negligible memory footprint.

### A.5 Additional Results on the Recall Metric

In the experiments (Sec. 4.2), we showed that our approach outperforms all other baselines on the mAP@ $k$ . However, other metrics like Recall@ $k$  are also common in the VPR literature. In Fig. 9, we show that the same trends are observed as in Sec. 4.2 on the Recall@ $k$  metric as well. We demonstrate the VPR performance on two datasets using the Dino embedding.

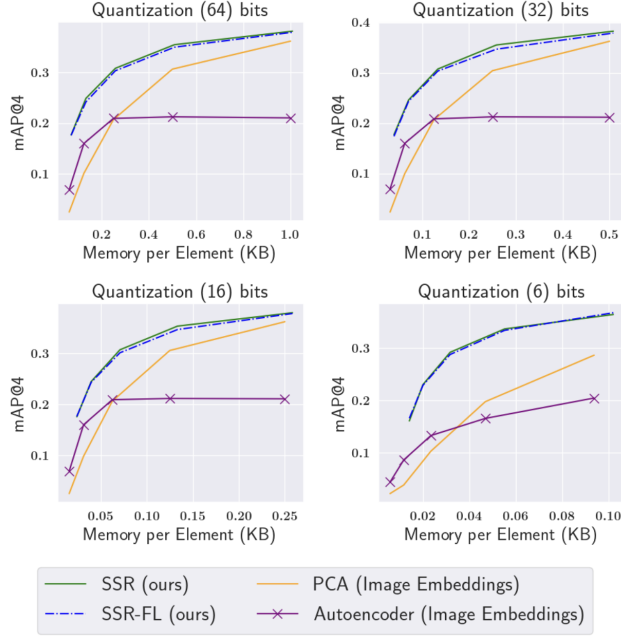


Figure 8: **SSR and SSR-FL are orthogonal to quantization.** We compare the performance of various baselines across different quantization levels. Our approach outperforms all baselines at each quantization level. While methods such as PCA and Autoencoders experience significant performance drops at 6-bit quantization, SSR and SSR-FL maintain stable performance.

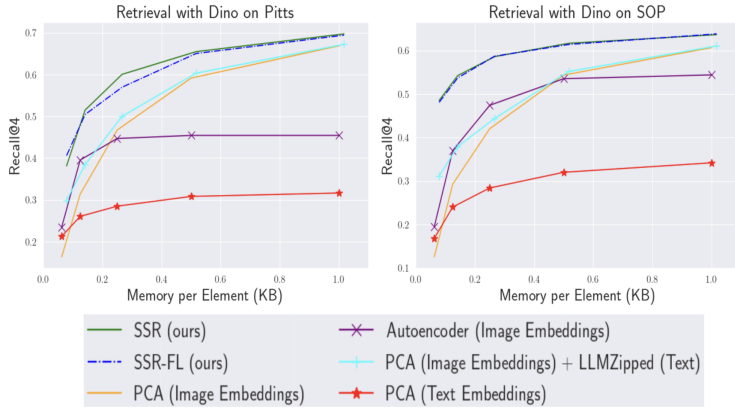


Figure 9: **Additional results on the Recall@ $k$  metric.** We see the same trends as in the main paper and we outperform all other baselines on the Recall@ $k$  metric

### A.6 Additional Results with JPEG and JPEG2000

In the experiments (Sec. 4.2), we did not report the performance of JPEG and JPEG 2000 as they were not comparable to the other baselines. Table 2 presents the memory footprint required to achieve a given VPR performance. As shown, SSR requires approximately  $10\times$  less data to achieve the same VPR performance as JPEG and JPEG 2000.

### A.7 Other Details

All baselines requiring training were trained for 5 epochs with a learning rate of  $10^{-4}$ . For SSR-FL, we utilized 4 nodes in a federated learning (FL) setup. The training data was randomly split across these 4 nodes. We assumed the presence of a central server to orchestrate the FL training process.

	JPEG	JPEG 2000	SSR
map@4 = 0.2	0.1	0.09	<b>0.01</b>
map@4 = 0.4	1.1	0.9	<b>0.1</b>

Table 2: Memory footprint of JPEG, JPEG 2000, and SSR required for given VPR performances.

However, this central server assumption is not critical to our approach, as SSR-FL can also be trained in a decentralized FL setup.